

Gaussian-Charge Polarizable Interaction Potential for Carbon Dioxide

Rasmus A. X. Persson^{1, a)}

Department of Chemistry, University of Gothenburg, Sweden

A number of simple pair interaction potentials of the carbon dioxide molecule are investigated and found to underestimate the magnitude of the second virial coefficient in the temperature interval 220 K to 448 K by up to 20%. Also the third virial coefficient is underestimated by these models. A rigid, polarizable, three-site interaction potential reproduces the experimental second and third virial coefficients to within a few percent. It is based on the modified Buckingham exp-6 potential, an anisotropic Axilrod-Teller correction and Gaussian charge densities on the atomic sites with an inducible dipole at the center of mass. The electric quadrupole moment, polarizability and bond distances are set to equal experiment. Density of the fluid at 200 and 800 bars pressure is reproduced to within some percent of observation over the temperature range 250 K to 310 K. The dimer structure is in passable agreement with electronically resolved quantum-mechanical calculations in the literature, as are those of the monohydrated monomer and dimer complexes using the polarizable GCPM water potential. Qualitative agreement with experiment is also obtained, when quantum corrections are included, for the relative stability of the trimer conformations, which is not the case for the pair potentials.

PACS numbers: 61.20.Ja 61.46.Bc 65.20.-w

^{a)}Electronic mail: rasmus.persson@chem.gu.se

I. INTRODUCTION

For carbon dioxide (CO_2), being an important industrial chemical, numerous interaction potentials (IPs) have been proposed, surpassed perhaps only by water in the amount of computer attention it has attracted among the molecular models. There are the parametric fits to the *ab initio* potential energy surface of the dimer, such as the the IPs of Steinebrunner and coworkers,¹ of Bukowski and colleagues,² and of Bock *et al.*³ The most successful and widely used IPs, however, have been fitted against bulk properties known from observation, such as the vapor-liquid equilibrium⁴⁻⁶ (VLE) or the crystal lattice parameters⁷, and still others against experimental properties of the dilute gas, such as the second virial coefficient.^{8,9} One may ask why this is so, but the *ab initio* IPs employ a great number of fitting parameters, not always of clear physical origin and, even so, interfacing them with other IPs, for instance when studying mixtures, is technically difficult because suitable combining equations are not known for the many parameters. Moreover, this problem is not unique to the *ab initio* IPs: also some empirical IPs use truncated series expansions^{5,8,9} for both angular and radial functions in a way which makes it difficult to interface them with IPs of radial site-site interactions. Hence, such IPs can find little use outside simulations of the neat liquid. On the other hand, great success has been enjoyed by the simple site-site interaction formula of one Lennard-Jones interaction center, and one atomic point charge, centered on every atomic site^{4,6,7,10}. Restricting ourselves to the rigid models, these can all be regarded as descendants of the original⁷ IP due to Murthy, Singer and MacDonald (MSM). These IPs have the very appealing property that they can be readily interfaced (“mixed”) with existing force fields, many of which share the exact same mathematical form.

Nature is not kind enough, however, to allow such a simplified description of the CO_2 molecule at no cost. Even though very good experimental agreement for a wide variety of properties is obtained by the simple, rigid model with three Lennard-Jones centers and one point quadrupole developed by Merker *et al.*,¹¹ like the EPM-2 model,¹⁰ it suffers from experimental disagreement in more “basic” properties such as the carbon-oxygen bond distance. With respect to the VLE envelope, the most successful such simple MSM-type model to date is the IP due to Zhang and Duan⁶ (ZD). Nevertheless, despite its high accuracy in this property, I report in this Note that the microstructure of the dimer, and the temperature dependence of the second, $B_2(T)$, and third, $B_3(T)$, virial coefficients are of much poorer

quality. It should be pointed out, also, that the results presented in Ref. 6 have been called into question.¹²

One striking omission from the published CO₂ IPs is that of many-body effects. That the CO₂ molecule lacks an electric dipole moment may have dissuaded investigators from looking in this direction, but in the work leading up to this Research Note, extensive trials indicated that it is not possible with a non-polarizable IP of MSM-type to simultaneously fit $B_2(T)$ while keeping the experimental agreement of the VLE envelope, at least not if the experimental bond distance and electric quadrupole moment are to be kept intact. The decision was then made in favor of a polarizable IP, to be described in this Note, but the extra cost that the high-resolution solution of the electric field equations incurs, even for a single polarization site, make simulations of the vapor-liquid coexistence prohibitively expensive for parametrization purposes. Instead, the temperature-dependence of the fluid density at 200 bar was used as a test for the many-body (concentrated phase) and $B_2(T)$ for the two-body (dilute phase) properties. Further developments then introduced a three-body dispersion interaction of Axilrod-Teller type,¹³ and $B_3(T)$ as a parametrization target. As a test of the validity of the IP, numerous other properties are calculated without input into the parametrization procedure. The model introduced in this work goes by the moniker of Gaussian Charge Polarizable Carbon Dioxide (GCPCDO). This is because of its great similarity to the highly successful GCPM water¹⁴ from which it borrows most of the essential equations.

This Note is organized as follows. First, in Section II a description of the mathematical form of the IP is given, and also the details of the calculations and the targeted properties of the parametrization. Then in Section III, the results are presented and discussed. Finally, a brief recapitulation of the main points is given in Section IV.

II. MODEL AND COMPUTATIONAL DETAILS

A. Electrostatic interaction

We compute the interaction between partial charge q_α and partial charge q_β at a separation of $r_{\alpha\beta}$, through the formula

$$u_q(r_{\alpha\beta}) = \frac{q_\alpha q_\beta}{r_{\alpha\beta}} \eta(r_{\alpha\beta}, \tau_\alpha, \tau_\beta) \quad (1)$$

Here $\eta(r_{\alpha\beta}, \tau_\alpha, \tau_\beta)$ is a function that assures that the electrostatic interactions remain finite at all separations; for large $r_{\alpha\beta}$ it approaches unity. Physically, this corresponds to charges distributed over a finite volume in space and like this we avoid the singularity of the potential at zero charge separation. For point charges, η is identical to unity and Eq. (1) reduces to the classical Coulomb law. We choose the following form for the η -function,

$$\eta(r_{\alpha\beta}, \tau_\alpha, \tau_\beta) = \operatorname{erf} \left(\frac{r_{\alpha\beta}}{\sqrt{2(\tau_\alpha^2 + \tau_\beta^2)}} \right) \quad (2)$$

which corresponds the physical case of two Gaussian charge distributions of standard deviations τ_α and τ_β interacting with each other.¹⁵

For now, we shall not concern ourselves with the general case of many-body interaction, as given by both “static” and “dynamic” electron correlation, but exclusively take care of that “static” correlation from the average electric field around each molecule, *i. e.* electronic induction effects. Furthermore, we do not carry this analysis beyond the dipole induction, *i. e.* we consider only the gradient of the electric potential. An induced dipole is hence positioned at the center of mass of molecule l and is given by

$$\vec{\mu}_l = \vec{E}_l (\alpha_\perp + |\cos(\theta)|(\alpha_\parallel - \alpha_\perp)) \quad (3)$$

where \vec{E}_l is the electrostatic field at that point, α_\perp the polarizability perpendicular to the molecular axis and α_\parallel that parallel to the same. Both α_\perp and α_\parallel are known from theory¹⁶ and their average agree in magnitude with that ascertained in experiment,^{17,18} but the interpolation between them has been chosen merely for convenience. θ is the angle between the molecular axis and the direction of \vec{E}_l , the electric field at site l . Because of the uncertainty in the precise form of the polarization matrix, and the approximations involved with the rigid rotor, the polarizabilities have been rounded to only two significant digits. In its turn, the electric field is computed as the sum of the contributions due to the permanent charges and that due to the other induced dipoles,

$$\vec{E}_l = \vec{E}_l^q + \vec{E}_l^\mu \quad (4)$$

where \vec{E}_l^q is the electric field at the center of molecule i due to the all the charges on the other molecules, and \vec{E}_l^μ is the electric field at the same point, but due to all the other induced dipoles. These are given by

$$\vec{E}_l^q = \sum_{m \neq l} \sum_{\beta \in m} \frac{q_\beta (\vec{r}_l - \vec{r}_\beta)}{r_{l\beta}^3} \left(\eta(r_{lm}, \tau_l, \tau_\beta) - \frac{\partial}{\partial r_{lm}} \eta(r_{lm}, \tau_l, \tau_\beta) \right) \quad (5)$$

and

$$\vec{E}_l^\mu = \sum_{m \neq l} \mathbf{T}_{lm} \vec{\mu}_m \quad (6)$$

where the tensor \mathbf{T}_{lm} is obtained from the Hessian of equation (1), with – following Paricaud *et al.*¹⁴ – the charge width parameter of the molecular center equal to that of the center atom. If the dipoles are converged, the extra energy of interaction due to the polarization is given by,¹⁹

$$U_{\text{pol}} = -\frac{1}{2} \sum_{l=1}^N \vec{\mu}_l \cdot \vec{E}_l^{\text{q}} \quad (7)$$

B. Dispersion interaction

First of all, the modified Buckingham exp-6 potential is adopted between atoms α and β ,

$$u_{\text{disp},2}(r_{\alpha\beta}) = \frac{\epsilon_{\alpha\beta}}{1 - 6/\gamma_{\alpha\beta}} \left[\frac{6}{\gamma_{\alpha\beta}} \exp \left\{ \gamma_{\alpha\beta} \left(1 - \frac{r}{\sigma_{\alpha\beta}} \right) \right\} - \left(\frac{\sigma}{r} \right)^6 \right] \quad (8)$$

This represents the pairwise additive part of the dispersion interaction as well as the steric repulsion between atoms. Also for this interaction, a hard-core is introduced at $r_{\alpha\beta} = 0.57\sigma_{\alpha\beta}$ to avoid the spurious behavior of this potential at short range. This is the same hard-core cutoff used by Paricaud and coworkers¹⁴ in the GCPM water model. Investigations indicated that the results are not very sensitive to the shortening of this hard-core radius to $0.35\sigma_{\alpha\beta}$, but the speed of simulation is. Here $\epsilon_{\alpha\beta}$, $\gamma_{\alpha\beta}$ and $\sigma_{\alpha\beta}$ are atomic interaction parameters, related to the well-depth, steepness and position, respectively, of the dispersion interaction. Second, a modified Axilrod-Teller term is added for all molecular triples. This is the triple-dipole dispersion correction to the van der Waals interaction which was first published by Axilrod and Teller.¹³ In the derivation by Axilrod,²⁰ spherical polarizabilities are assumed, but for anisotropically polarizable molecules, such as CO_2 , his result does not hold. To investigate this case, we quickly recapitulate Axilrod’s derivation²⁰ where we dispose of the assumption of spherical polarizabilities.

For each of the three molecules l , m and n , we define a local coordinate system where the z -axis is normal to the plane of the molecular centers, the x -axis parallel to the bisector of the angle spanned by the two other molecules and the y -axis mutually orthogonal to the x - and z -axes. Hence, the z -axes all coincide between the three local coordinate systems, but the x - and y -axes need not. Assume now that the electronic structure of each molecule

is independent and described by a wavefunction that factorizes into separable x -, y - and z -contributions in its local coordinate system, *i. e.* for molecule l ,

$$\psi_l(x_l, y_l, z_l) = X(x_l)Y(y_l)Z(z_l) \quad (9)$$

We write the third-order perturbation correction to the groundstate energy, W_0''' , which in Axilrod's notation is (Eq. [5a] in Ref. 20),

$$W_0''' = \sum_j \sum_{\substack{k \\ j \neq k, 0 \\ k \neq 0}} \frac{H'_{0j} H'_{jk} H'_{k0}}{(W_j^0 - W_0^0)(W_k^0 - W_0^0)} \quad (10)$$

Here H'_{jk} is the matrix element of the dipole perturbation for states j and k , and W_j^0 is the energy of state j . Invoking the closure approximation,²¹ this equation may be approximately recast as

$$W_0''' \approx \frac{1}{\nu'} \sum_j \sum_{\substack{k \\ j \neq k, 0 \\ k \neq 0}} H'_{0j} H'_{jk} H'_{k0} \equiv u_{\text{disp},3}(l, m, n) \quad (11)$$

where

$$\nu' = \langle (W_j^0 - W_0^0)(W_k^0 - W_0^0) \rangle_{jk} \quad (12)$$

and $\langle \dots \rangle_{jk}$ signifies the arithmetic average over j and k . Eq. (11) serves to define the three-body correction to the dispersion energy that we will use.

Formally, the set of matrix elements $\{H'_{jk}\}$ covers all possible excited states but we shall assume contributions to the sum only from the first excited orbital of each symmetry for each molecule. That is, the three lowest excited states of the arbitrary molecule l are assumed to be $X^*(x_l)Y(y_l)Z(z_l)$, $X(x_l)Y^*(y_l)Z(z_l)$ and $X(x_l)Y(y_l)Z^*(z_l)$ where the asterisk denotes the next higher-energy orbital. Because they share a common orthogonal z -axis, only mixed excited states for x - and y - components between the molecules contribute to the sum over states. Hence, the matrix elements for the sequences of possible excitations are exhaustively given in Table I of Ref. 20 and the explicit form of these matrix elements is provided in Eq. (29) of the same reference, except that the common factor M^2 is no longer applicable because the transition diople moment is no longer the same for the different components. Instead, given the two molecules l and m , excited in their x and y orbitals, respectively, we write the corresponding matrix element (*cf.* Eq. [29] in Ref. 20)

$$(x_m, y_l) = (M_{x_m} M_{y_l} / (4\pi\epsilon R_{ml}^3)) (2 \cos \frac{1}{2}\gamma_m \sin \frac{1}{2}\gamma_l - \sin \frac{1}{2}\gamma_m \cos \frac{1}{2}\gamma_l) \quad (13)$$

where M_{x_m} denotes the expectation value of transition dipole moment along the x -axis of molecule m and γ_m the angle defined by the molecules l , m and n with its the apex in molecule m . All the other matrix elements follow by analogy with Ref. 20. We have written Eq. (13) in a general form with ε being the permittivity of the medium in which the molecules are dispersed. It is most reasonable to take this as the permittivity of free space. Since because of the very short-range nature of the interaction (it tapers off as the inverse ninth power of distance) it is unreasonable to assume that a homogeneous medium of CO₂ molecules can be accommodated between the interacting molecules. The final approximation is to replace the M -factors by the square-root of the corresponding polarizabilities. Collecting the constants of proportionality in the common prefactor of Eq. (11), which is then seen to have dimensions of reciprocal energy, we treat it as a fitting parameter and denote it by $1/\nu$ proper.

With anisotropic polarizabilities, the sum over states in Eq. (11) does not simplify to the simple form given in the original references^{13,20} and the complicated closed-form expression will not be reproduced here. In any case, since it involves sines and cosines it is not optimal from a computational point of view; it is much more efficient in terms of the total number of floating-point operations to calculate the truncated sum over states directly. To this end, the half-angle formulas are used to rewrite the matrix elements, such as the one in Eq. (13), in terms of dot products and square-roots, which are much more efficient in terms of CPU cycles than trigonometric functions. The polarizabilities are calculated, like before, as the interpolation

$$\alpha(\theta) = \alpha_{\perp} + |\cos(\theta)|(\alpha_{\parallel} - \alpha_{\perp}) \quad (14)$$

where θ is, once again, the angle to the molecular axis. The limiting polarizabilities are taken to be the same as the static ones.

In total, after self-consistent solution of the induced dipoles, the energy of interaction among N molecules is given by

$$U = \sum_{l=1}^N \sum_{m>l}^N \sum_{\alpha \in l} \sum_{\beta \in m} (u_q(r_{\alpha\beta}) + u_{\text{disp},2}(r_{\alpha\beta})) - \frac{1}{2} \sum_{l=1}^N \vec{\mu}_l \cdot \vec{E}_l^q + \sum_{l=1}^N \sum_{m>l}^N \sum_{n>m}^N u_{\text{disp},3}(l, m, n) \quad (15)$$

The analytical gradient of this expression is very involved, with the chain-rule giving factors proportional to the gradient of the polarizability. Consequently, when the gradient has been needed, for instance, in energy minimization, it has been calculated numerically using the finite-difference approximation.

C. Parametrization strategy

1. Gas-phase properties

A number of parameters have not been optimized, but simply assigned from plausible experimental values in the literature. Thus, the bond length is fixed at 1.161 Å, midway between published values of 1.160 Å and 1.162 Å by experimental groups,^{22,23} and the partial charges on the atoms are chosen to reproduce the experimental quadrupole moment.^{24,25} To further reduce the number of free parameters, the charge width of the oxygen atom, τ_{O} , was set equal to 0.610 Å, the value of the oxygen atom in GCPM water,¹⁴ and, the corresponding quantity for carbon was scaled according to the ratio of the σ parameters (*vide infra*). These parameters were not optimized. Moreover, I introduced the additional constraint of $\gamma_{\alpha\alpha} = \gamma_{\beta\beta} = \gamma_{\alpha\beta}$ and for the remaining parameters, the following “mixing rules” were adopted for unlike interactions of the modified Buckingham exp-6 potential,

$$\epsilon_{\alpha\beta} = \frac{2\epsilon_{\alpha\alpha}\epsilon_{\beta\beta}}{\epsilon_{\alpha\alpha} + \epsilon_{\beta\beta}} \quad (16)$$

$$\sigma_{\alpha\beta} = \frac{1}{2}(\sigma_{\alpha\alpha} + \sigma_{\beta\beta}) \quad (17)$$

Eq. (16) can be justified with appeal to the London formula,²⁶ in which the harmonic average of the ionization energy is taken. Normally, it is the geometric average of the polarizabilities in said equation that lends its mathematical form to the combining rule for the ϵ -parameters. However, the precise form of the mixing rules are of a secondary concern, as they serve mainly to reduce the parameter space that has to be fit, and provided the atomic interaction parameters do not turn out to be very different from each other, the result will be insensitive to reasonable choices of mixing rules.

A test set of potentials with predefined σ values, covering a broad range, but with the ratio, $\sigma_{\text{C}}/\sigma_{\text{O}}$ of the carbon sigma value, σ_{C} , and the oxygen sigma value, σ_{O} , conserved at 1.0483 were investigated. This value was arbitrarily chosen early in the development of the model and never subjected to revision. For each such class of IPs, manual tuning of the ϵ -parameters in trial-and-error fashion was made to obtain a good fit for $B_2(T)$ against experimental data and a reasonable binding energy and geometry of the dimer structure. $B_2(T)$ was calculated from the Mayer sampling method²⁷ over 5×10^8 Monte Carlo steps. Typically, with this number of Monte Carlo steps, the resulting uncertainty, calculated from

the block average method²⁸ with blocks of 10^5 cycles, is of the order of one percent. The induced dipoles were iteratively solved to within a tolerance of 3×10^{-10} D at all times. In the course of this parametrization, it was found that the γ -parameter plays a most crucial role. This parameter controls the steepness of the modified Buckingham potential, without affecting well depth or location. Small values lead to a flat minimum and $B_2(T)$ turned out to be very sensitive to this parameter. Thus, it was found that, to fit $B_2(T)$, this parameter had to be increased from its initial estimate of 12.75 (taken from GCPM water¹⁴) to 15.50.

Later in the development of the model, it was found necessary, with respect to the liquid densities, to include also the three-body dispersion in the energy expression. Because the ν -parameter is completely independent of all dimer properties, including $B_2(T)$, it was fitted independently so that $B_3(T)$ coincided with the data of Dushek *et al.*,²⁹ It was not possible to reproduce, with this single parameter, also the data of Holste *et al.*,³⁰ something which lends credence to the former measurements. The value obtained, $\nu = 2.82 \times 10^4$ K, is reasonable in that it is of the same order of magnitude as the Axilrod-Teller coefficient obtained for argon, for which this coefficient is 2.1×10^4 K in the appropriate units.³¹

2. Bulk simulations

The fluid densities were extracted from isothermal-isobaric Metropolis Monte Carlo simulations³² for an ensemble of 200 molecules in periodic boundary conditions of cubic symmetry over $M = 2.5 \times 10^7$ steps, run in parallel over five independent Markov chains. Standard errors of the mean were estimated from the block average method²⁸ with \sqrt{M} blocks.

For the modified Buckingham potential, with neglect of interactions beyond the cutoff the energy was corrected by

$$U_{\text{LRC}} = u_{\text{LRC}}^{\text{CC}} + 4u_{\text{LRC}}^{\text{CO}} + 4u_{\text{LRC}}^{\text{OO}} \quad (18)$$

where $u_{\text{LRC}} = \frac{\rho}{2} \int_{r_c}^{\infty} 4\pi r^2 U_{\text{exp-6}}(r) dr$ and superscripts indicate between which two atom types the interaction is computed. Here ρ is the number density of molecules. The integral in question can be analytically computed, which yields

$$u_{\text{LRC}} = \frac{2\pi\epsilon\rho}{1 - 6/\gamma} \left[\frac{6\sigma}{\gamma^4} (r_c^2\gamma^2 + 2r_c^2\gamma\sigma + 2\sigma^2) \exp\left(\gamma - \frac{r_c\gamma}{\sigma}\right) - \frac{\sigma^6}{3r_c^3} \right] \quad (19)$$

For the Axilrod-Teller terms, in light of their very strong distance dependence, no long-range correction was deemed necessary.

For the electrostatic interaction, a long-range correction was introduced for the induced dipole using the Onsager expression for the dipole reaction field³³ with the dielectric constant taken from the Clausius-Mosotti equation fitted against experimental measurements of the dielectric constant.³⁴ This may seem to be very approximate but was done for two principal reasons. First, lattice summation techniques such as the Ewald sum³⁵ introduce assumptions of periodicity which are unsuitable for the uncorrelated nature of the molecules in a disordered phase. Second, the quadrupolar interaction terms decay sufficiently fast with distance so as to make their sum absolutely convergent. On the assumption of uncorrelated molecules beyond the cutoff radius, the long-range correction vanishes. Last but not least, the exact same procedure was used by Paricaud *et al.* in their simulations of GCPM water.¹⁴ As a technical side-note, it should be pointed out that Ewald summation for Gaussian charges is complicated by the fact that the required Fourier transform for the reciprocal space sum is not analytically tractable. Using the reciprocal space sum for point charges, with due corrections in direct space and a long cutoff radius, is an alternative but inefficient.

Each trial move consisted of randomly displacing and rotating from one up to four molecules. Interaction cutoffs were introduced at half the box length. For the three-body dispersion, this was interpreted to mean that all interacting molecules had to be within cutoff of each other. Simple mixing³⁶ with a mixing factor of 10% was used to enforce and speed convergence. Because of increased computational load, the induced dipoles were solved to within a tolerance of 3.4×10^{-5} D per molecule. This is still less tolerant than many other reported simulations of polarizable IPs: Ren and Ponder³⁷ report simulations on liquid water with their AMOEBA force field where the dipoles are solved to within 10^{-2} D precision; Paricaud *et al.*¹⁴ solve the induced dipoles to within 5×10^{-5} D in their simulations of GCPM water. However, further relaxation of the tolerance is unnecessary as the greater part of the simulation time is not spent on the self-consistent solution of the electrostatic field equations, but (about 70%) on the evaluation of $\sum_{lmn} u_{\text{disp},3}(l, m, n)$. This computation can be significantly sped up with shorter interaction cutoffs.

Two types of bulk simulations were performed. A series of NpT -simulations to determine the density and constant-pressure heat capacity of the model fluid and NVT -simulations to

determine the radial distribution functions of the model fluid. Together with the calculation of the virial coefficients, these served to parametrize the model. All parameters except for ν were decided for the potential model lacking the u_3 term, which has no effect on either the dimer binding energy, its geometry or the second virial coefficient. Selection among candidates of this pairwise dispersion model was effected by comparing densities from the NpT -simulation with experiment, although the long-range correction was not fully developed at this time. Subsequent introduction of the long-range correction lead to an increase of the computed densities, later corrected by the introduction of the three-body dispersion interaction. The final parameters, extracted from these tests, are listed in Table I.

III. RESULTS AND DISCUSSION

A. Virial coefficients

Not only have calculations for the parametrization of the GCPCDO IP been carried out, but in the investigations leading up to its formation, I also investigated some other CO₂ IPs. The VLE envelopes of these models have all been thoroughly investigated in Ref. 6, in which it was established that the ZD potential exhibits near-perfect experimental agreement in this property. While this excellent agreement might not be reproducible in every aspect,¹² the critical temperature and density cannot lie very far from their experimental counterparts nonetheless, because the relative deviations between the coexistence densities reported in Ref. 6 and Ref. 12 decrease and approach the experimental values when nearing the experimental critical temperature. Moreover, the variation in $B_2(T)$ is not very great between the models; except possibly for the TraPPE IP³⁸ which—it is interesting to point out—is that of the non-polarizable IPs of MSM-type, which exhibits the best experimental agreement for both $B_2(T)$ and $B_3(T)$. For the GCPCDO IP, having had this as one of its goals in the parametrization, the fit is very good with the relative error never exceeding 5%. The results are reported for a select number of temperatures in Table II.

It does seem surprising that IPs that fare very well in reproducing VLE properties should fail so remarkably at reproducing the much “simpler” property $B_2(T)$. If $B_2(T)$ is overestimated, then a compensating underestimation of $B_3(T)$ seems very likely. Direct calculation

TABLE I. Interaction parameters and experimental observables for the GCPCDO model and, where appropriate, experimental reference values.

Parameter	GCPCDO	Exp.
$\sigma_{\text{O}} / \text{\AA}$	3.347	
$\sigma_{\text{C}} / \text{\AA}$	3.193	
$\epsilon_{\text{O}} / \text{K}$	67.72	
$\epsilon_{\text{C}} / \text{K}$	71.34	
ν / K	2.82×10^4	
$\gamma_{\text{O}} / \text{\AA}$	15.50	
$\gamma_{\text{C}} / \text{\AA}$	15.50	
$\tau_{\text{O}} / \text{\AA}$	0.6100	
$\tau_{\text{C}} / \text{\AA}$	0.5819	
q_{O} / e	-0.3321	
q_{C} / e	0.6642	
$\alpha_{\perp} / \text{\AA}^3$	1.95	1.929 ^a
$\alpha_{\parallel} / \text{\AA}^3$	4.05	4.038 ^a
Bond length / \AA	1.161	1.160 ^b
		1.162 ^c
Quadrupole / ($e \text{\AA}^2$)	-0.90	-0.85 ^d
		-0.90 ^e
		-0.96 ^e

^a Ref. 17

^b Ref. 22

^c Ref. 23

^d Ref. 24

^e Ref. 25

of $B_3(T)$ for the computer models seem to confirm this. However, contrary to the case of $B_2(T)$, good quality experimental data are very hard to find for $B_3(T)$. Different authors report widely different results, over the same temperature range. In the narrow range around the critical temperature, however, both Holste *et al.*³⁰ and Dushek *et al.*²⁹ report measure-

TABLE II. Second virial coefficients for the ZD, MSM, EPM2, TraPPE and GCPCDO IPs, as well as experimental results, at a select number of temperatures. For the computed results, bracketed numbers indicate the estimated standard error of the mean in the last digit from the Mayer sampling²⁷ Monte Carlo integration.

$B_2 / (\text{cm}^3 \text{ mol}^{-1})$						
T / K	ZD	MSM	EPM2	TraPPE	GCPCDO	Exp.
220.00	-200.6(6)	-204.7(6)	-206.6(7)	-222.0(7)	-247.2(9)	-247.50 ^a -247.52 ^b
240.00	-168.1(5)	-171.5(6)	-170.9(6)	-183.5(6)	-202.8(9)	-202.83 ^a -202.13 ^b
260.00	-141.7(5)	-145.0(5)	-144.7(5)	-153.7(6)	-169.8(9)	-168.92 ^a -168.27 ^b
280.00	-120.6(5)	-123.3(5)	-122.1(5)	-129.3(5)	-143.7(7)	-142.70 ^a -142.11 ^b
300.00	-104.4(4)	-106.2(4)	-105.0(4)	-110.3(5)	-123.5(6)	-121.70 ^a -121.35 ^b
340.00	-78.0(4)	-79.5(4)	-78.0(4)	-81.9(4)	-91.3(4)	-90.57 ^b
423.15	-43.5(3)	-44.8(3)	-43.8(3)	-45.6(4)	-52.2(4)	-51.25 ^a
448.15	-36.6(3)	-37.5(3)	-36.5(3)	-37.7(3)	-43.9(3)	-43.51 ^a

^a Ref. 30

^b Ref. 29

ments which are in at least slight mutual concordance. In Table III, these measurements are reported and compared with predictions from the IPs. As is evident, the pairwise additive IPs underestimate $B_3(T)$ across the whole temperature range.

B. Volumetric properties

To investigate the properties of the many-body potential with more than just three bodies, the density and the heat capacity at constant pressure, both readily extracted from the NpT simulations, serve as indicators. These results are summarized in Table IV with ex-

TABLE III. Third virial coefficients for the ZD, MSM, EPM2, TraPPE and GCPCDO IPs, as well as experimental results, at a select number of temperatures. For the computed results, bracketed numbers indicate the estimated standard error of the mean from the Mayer sampling²⁷ Monte Carlo integration.

T / K	$B_3 / (\text{cm}^6 \text{ mol}^{-2})$					Exp.
	ZD	MSM	EPM2	TraPPE	GCPCDO	
280.00	2920(30)	2940(30)	2910(30)	3080(40)	5140(60)	5636 ^a 5165 ^b
300.00	2820(20)	2860(20)	2922(20)	3060(30)	4790(60)	4927 ^a 4753 ^b
320.00	2690(20)	2760(20)	2700(20)	2870(20)	4460(50)	4423 ^a 4360 ^b
340.00	2530(20)	2570(20)	2560(20)	2680(20)	4046(50)	3996 ^b

^a Ref. 30

^b Ref. 29

perimental data. It is surprising that the agreement with experiment is considerably better at the higher densities. This increasing discrepancy between theory and experiment can be tentatively attributed to the fourth virial coefficient, $B_4(T)$. It is clear that in order to explain these results, $B_4(T)$ (or possibly higher virial coefficients) must rise quicker with temperature for the GCPCDO model than for its experimental counterpart. Unfortunately, quality experimental values of $B_4(T)$ are not known but it is worth pointing out that if one applies the virial equation of state truncated after $B_3(T)$, the computed densities at 290 K and 310 K turn out to be $0.915 \pm 0.018 \text{ g / cm}^3$ and $0.791 \pm 0.015 \text{ g / cm}^3$, respectively, at 200 bar pressure. These values are indeed very close to the simulated values reported in Table IV and indicate that $B_4(T)$ is overestimated and close to zero. However, because at the higher pressure, the truncated virial equation of state predicts densities *higher* than the simulated ones, it is clear that higher-order coefficients must be compensating for errors in $B_4(T)$. This is not surprising, at high densities, the steric effects become the dominant mode of interaction. Sadly, the precise causes of these deviations in the virial coefficients is unknown. Unlike the other models investigated in this work, we have come some way in

correcting $B_2(T)$ and $B_3(T)$ to their correct experimental values. However, we may safely say that the interactions of the CO_2 molecule are not as simple as one may at first suppose.

Also shown in Table IV is the constant-pressure heat capacity which was calculated from the fluctuation formula,³⁹

$$C_p = \frac{1}{NkT^2} (\langle H^2 \rangle - \langle H \rangle^2) \quad (20)$$

where $H = U + pV + 5kT/2$ is the enthalpy, the last term being the classical kinetic contribution of a linear rigid body and k the Boltzmann constant, p the pressure, U the potential energy, V the volume, N the number of molecules and T the temperature. For a completely fair comparison with the experimental values, also the internal vibrational degrees of freedom should be included. Assuming harmonic behavior, for each normal mode of frequency ν this quantized harmonic contribution to the heat capacity is then

$$C_{p,h} = k \left(\frac{h\nu}{kT} \right)^2 \left(\exp \left(\frac{h\nu}{kT} \right) - 1 \right)^{-2} \exp \left(\frac{h\nu}{kT} \right) \quad (21)$$

where h is the Planck constant. Taking into account the experimental frequencies^{40,41} of the four harmonic normal modes of the CO_2 molecule, this term is added to C_p and reported as the corrected values in Table IV. Not surprisingly, this expression compares favorably with the experimental C_p extrapolated to vanishing density.⁴² For instance, the experimentally ascertained intramolecular contribution is 5.74 J / (K mol) at 250 K, whereas from Eq. (21) one has 5.78 J / (K mol). At 310 K, the experiments indicate 8.58 J / (K mol) and from Eq. (21) we have 8.68 J / (K mol). It is computationally too demanding, at present, to include the quantized vibrations in the bulk simulation of the GCPCDO IP and the approximation of separable internal and external degrees of freedom is expected to be fair.

The general overestimation of the heat capacity, even before the correction for intramolecular degrees of freedom, is due, at least in part, to the assumption of classical translational and rotational degrees of freedom. Especially at high density, free rotation and translation is not possible and the rotational and translational degrees of freedom are in effect partly quantized librational modes. Unlike the intramolecular degrees of freedom, these are highly coupled and there exists no viable computational approximation for their contribution to the heat capacity. The very large overestimation of the heat capacity at 310 K and 200 bar cannot, however, be attributed to this effect alone. Moreover, at this state point the discrepancy in density between real CO_2 and GCPCDO is so large that a more fair comparison

TABLE IV. Calculated and experimental fluid properties at 200 and 800 bar pressure and temperatures of 250 to 310 K. Heat capacities assume classical contribution of $3k$ for the rotational and translational degrees of freedom. The corrected heat capacities include the heat capacity of the quantized internal degrees of freedom within the harmonic approximation. For the calculated results, numbers in parentheses indicate the estimated standard error of the mean in the last digit.

p / bar	T / K	ρ / (g / cm ³)		C_p / (J / [K mol])		
		Calc.	Exp. ^a	Calc.	Corr.	Exp. ^a
200	250.0	1.100(4)	1.105	96(4)	102(4)	83.3
200	270.0	1.010(5)	1.032	87(3)	95(3)	86.0
200	290.0	0.902(7)	0.951	91(3)	99(3)	90.4
200	310.0	0.79(1)	0.856	109(5)	118(4)	97.7
800	250.0	1.216(2)	1.211	76(3)	82(2)	74.6
800	270.0	1.159(2)	1.165	71(2)	78(2)	73.7
800	290.0	1.107(2)	1.118	72(2)	80(2)	73.0
800	310.0	1.057(2)	1.073	68(2)	77(2)	72.4

^a Ref. 42

(as relates to C_p) is with the experimental C_p at 0.79 g / cm³ density, which is⁴² 119 J / (K mol), not too far off from the computed value.

No IP for the fluid can be deemed satisfactory if unable to reproduce the experimental fluid structure. Accordingly, at the density and temperature of the neutron-diffraction experiments of Cipriani *et al.*,⁴³ the atomic pair distribution functions (PDF), $g(r)$, have been computed, and these are shown in Figures 1 and 2 for two different thermodynamic states. What is experimentally ascertained, however, is not the individual, atomically resolved $g(r)$, but the superimposed effect from all atomic scatterers. Taking account not only of the four times greater abundance of C-O and O-O vectors than of C-C vectors between molecules, but also of the different propensity toward neutron scattering, the following formula was used to calculate the superimposed PDF,⁴⁴

$$G(r) = 0.403g_{OO}(r) + 0.464g_{CO}(r) + 0.133g_{CC}(r) \quad (22)$$

In terms of the position and number of peaks, these $G(r)$ are seen to be in reasonable-to-good

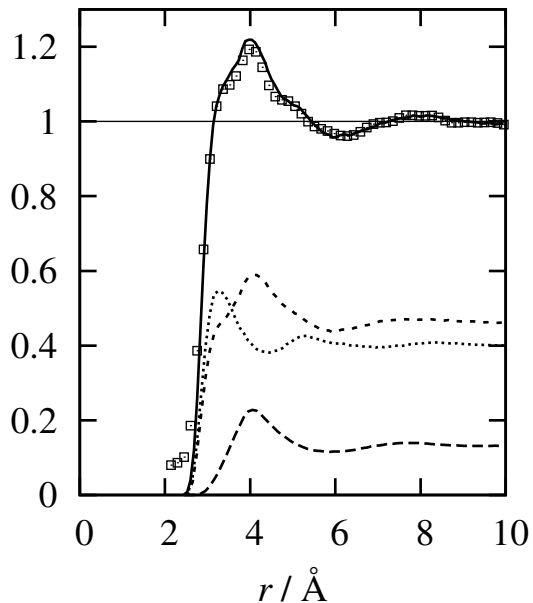


FIG. 1. The individual atomic PDFs, $g(r)$, of Eq. (22) for carbon-carbon (long-dashed line), carbon-oxygen (short-dashed line) and oxygen-oxygen (dotted line) at 312 K and 0.83 g / cm^3 for the GCPCDO IP as well as their superposition (full line), weighted by occurrence and scattering propensity, $G(r)$. Squares are experimental results from Ref. 43. For clarity, no intramolecular contributions are shown for the computed results.

agreement with the experimental results.

At 240 K and 1.09 g / cm^3 , the carbon-oxygen distribution function clearly shows more structure at short range, than at 312 K and 0.83 g / cm^3 , where the lack of orientational correlation in the fluid is also apparent in how quickly the atomic carbon-oxygen and oxygen-oxygen PDFs decay to unity. Still, however, the carbon-carbon PDF exhibits a slight peak at around 7.5 \AA indicating a weak second coordination shell, albeit of random order in molecular orientation. The PDFs indicate that the fluid is slightly overstructured at the higher density, where the first peak is overestimated. The better agreement for the computed PDF at the low density is most likely due to the overall lesser contributions from many-body effects at this density. For the pair potential used in Ref. 43, the first peak is overestimated at both thermodynamics states. Last, it should be pointed out that in the fluid with flexible bonds, a general broadening of the peak structure is expected. This effect is at least responsible for the deviation seen at the very short distances, where the internal scattering vectors

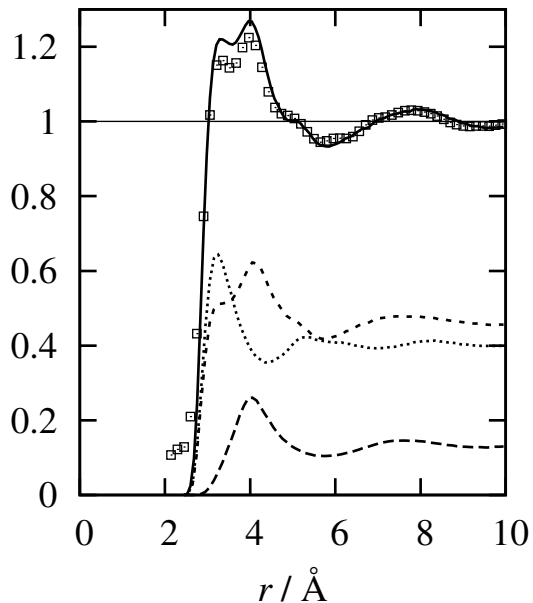


FIG. 2. Same as Figure 1 but for 1.09 g / cm^3 and 240 K .

contribute. In the rigid model, they are δ -functions and have been omitted for clarity.

C. Clusters

Having established the weakness of the GCPCDO model primarily in its $B_4(T)$, *i. e.* four-body interaction, we turn to properties of the IP for which only three bodies contribute. Clusters like these offer excellent tests of the model, due to the availability of quantum-mechanical reference calculations. It also allows us to pinpoint more clearly the role of many-body effects in the interaction potential.

1. Dimer and trimers

Both experiment^{45,46} and *ab initio* simulation¹⁻³ agree that the equilibrium dimer structure is of C_{2h} symmetry, with the *ab initio* simulations indicating that there is a saddle point of C_{2v} symmetry. The GCPCDO IP reproduces these two dimer states very well, as shown in Table V. As for the geometry of the dimer configurations (see Figure 3), it is neither better nor worse than the simpler ZD IP,⁶ but when it comes to the binding energy of the two states, it is markedly superior when judged against the *ab initio* IPs: the binding energy

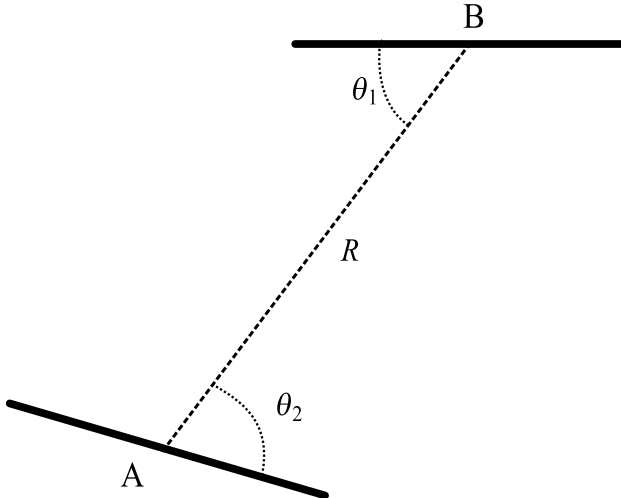


FIG. 3. Schematic illustration of the dimer with definitions of angles and distances. Each molecule is represented by a stick. All atoms lie in the same plane.

is underestimated by less than 4% for the minimum and overestimated by less than 1% for the saddle-point, whereas the ZD IP underestimates the binding energy in both cases by about 15–20%. This gross underestimation of the dimer binding energy helps explain the overestimation of $B_2(T)$ for the ZD model (*vide supra*) but is nevertheless surprising because for non-polarizable potentials the general trend is an overestimation of dimer binding energies.

Because the GCPCDO model is so successful at capturing the dimer binding energy, it is interesting to test it across a broader range of conformations. Hence, I show in Figure 4 the potential energy function of this model compared to the accurate data of the angular fit of the symmetry-adapted perturbation theory⁴⁷ calculations of Bukowski *et al.*,² the BUK IP, for radial displacements. Both the energy minimal pathway separating the two molecules and the path along the C_{2v} transition state are shown. For the energy optimal pathway, the optimized angles of the two molecules at each separation are shown in Table VI. The two molecules, for both the GCPCDO and BUK IPs, prefer a slipped-parallel conformation at close range, but eventually prefer the T-shaped geometry of the minimum at long range. The transition is noticeable as a slight trough in the dissociation curve at around 4 Å and

TABLE V. Equilibrium geometry and well-depth energy of the CO₂ dimer for the GCPCDO model, the ZD model, and BUK, the angular *ab initio* potential energy surface of Bukowski *et al.*² U refers to the potential well-depth at the specific conformation. See Figure 3 for the definitions of the geometric quantities.

	GCPCDO	ZD	BUK ^a	Exp. ^b
Minimum (C_{2h})				
U / K	-675.4	-548.7	-696.8	
θ_1, θ_2 / deg	55.5	56.5	59.0	57.96
R / Å	3.64	3.64	3.54	3.60
Saddle-point (C_{2v})				
U / K	-596.6	-508.7	-593.2	
θ_1 / deg	90.0	90.0	90.0	
θ_2 / deg	0.0	0.0	0.0	
R / Å	4.16	4.17	4.14	

^a Ref. 2

^b Ref. 46

is quicker for the BUK IP with an earlier onset.

Another interesting property of the model, which cannot be answered by the BUK IP, is the total dipole of the C_{2v} configuration. Because the electric field gradients are very inhomogeneous close to the molecule, it might be suspected that only allowing the center atom to polarize is artificially deflating the induced dipole, and like this introducing errors in the short-range interaction. For GCPCDO, the dipole is predicted to be 0.19 D at the transition-state separation. Running calculations with Gaussian 03,⁴⁸ the suspicion is confirmed as calculations of the dipole moment in the identical configuration at the CISD/aug-cc-pVDZ level of theory, predict a dipole moment of 0.21 D. The dipole moment is hence underestimated by 10% in the transition state configuration.

Because of its many-body nature, it is interesting to test the GCPCDO IP on the simplest cluster for which many-body effects contribute, *i. e.* the trimer. Consequently, energy minimized structures of the trimer have been located. The two most stable conformations are shown in Figures 5 and 6; the specific data on each are summarized in Table VII.

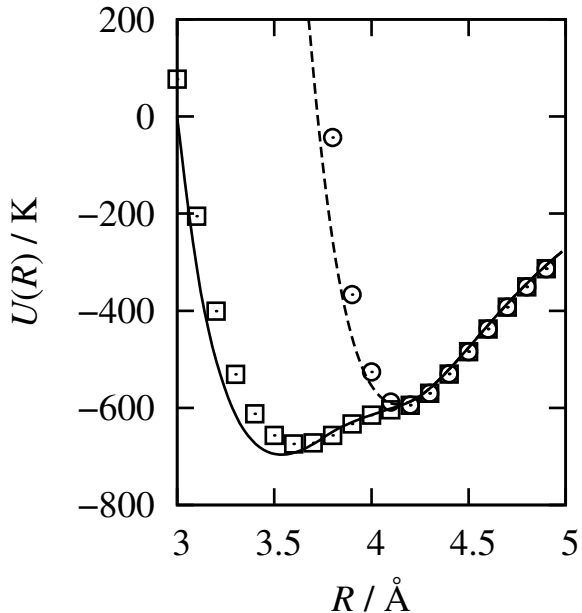


FIG. 4. Dependence of energy of interaction, $U(R)$, on separation, R , for two different paths of approach. Squares are for the energy minimal path of the GCPCDO IP and the full line is the analogous result for the BUK IP. Circles are for the C_{2v} conformation of the GCPCDO dimer, and the dashed line is for the BUK result.

Both of these trimer conformations have been observed spectroscopically, with the planar C_{3h} conformation being slightly more abundant.^{49,50} In terms of relative energies, however, neither of GCPCDO or BUK predict the right ordering, but there are two general remarks to be made. The first one is that the inclusion of many-body effects, clearly levels the difference between the two states, the difference in the GCPCDO prediction being less than 0.1 K.⁵¹ That many-body effects would alleviate the problem was hinted at already by Bukowski and coworkers² in their discussion of this problem and they argued using single-point calculation from higher-order quantum chemical theory that this was the case. Second, the possible role of the zero-point vibrational quanta has to be kept in mind. A first-order estimate of this effect is provided by the harmonic zero-point energy. Indeed, as indicated by Bukowski and coworkers,² inclusion of this energy for the BUK IP decreases the difference between the states. Carrying out the same analysis for the GCPCDO IP, however, we find that theory is brought into qualitative agreement with observation. As discussed by Bukowski and collaborators,² the harmonic approximation is very strained in the CO_2 trimer but correct evaluation of the zero-point vibrational energy necessitates a numerical solution of

TABLE VI. The optimum values of the angles θ_1 and θ_2 as a function of the separation R between two molecules as predicted by the GCPCDO IP and the BUK IP. The angles are defined geometrically in Figure 3.

$R / \text{\AA}$	GCPCDO		BUK	
	θ_1 / deg	θ_2 / deg	θ_1 / deg	θ_2 / deg
3.0	71.7	71.7	66.4	66.4
3.3	62.3	62.3	62.2	62.2
3.5	58.0	58.0	59.5	59.5
3.7	54.5	54.5	57.0	57.0
3.8	53.0	53.0	46.1	65.2
3.9	42.1	61.3	37.1	71.1
4.0	30.8	70.2	28.6	75.9
4.1	19.6	77.9	18.9	80.9
4.2	3.7	88.0	0.0	90.0
4.5	0.0	90.0	0.0	90.0

the Schrödinger equation. Future code development will remedy this situation. Even so, I believe that these results are indicative of the qualities of the GCPCDO IP.

2. *Water complexes*

Because of its transparent physical form, the GCPCDO IP can, through the adoption of suitable “combining rules”, be interfaced with other IPs. As a first test of the feasibility of this approach, I have calculated the binding energy and molecular geometry of the $[\text{H}_2\text{O}-\text{CO}_2]$ complex using the successful GCPM water¹⁴ for the water moiety. In addition to the combining rules of Eqs (16) and (17), the γ -parameters were calculated as

$$\gamma_{xy} = \frac{1}{2}(\gamma_x + \gamma_y) \tag{23}$$

For comparison purposes, the complexation of ZD CO_2 and TIP3P water⁵² serves as an indicator of the effect of neglected polarization. These results are summarized in Table VIII. It is important to point out that the potential energy surface of this complex is very

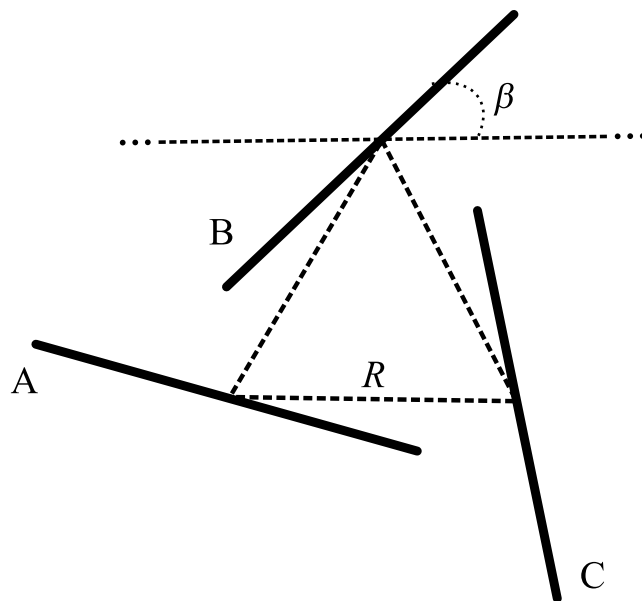


FIG. 5. Schematic illustration of the C_{3h} trimer. All atoms lie in the same plane. Molecules A, B and C are all identical by symmetry.

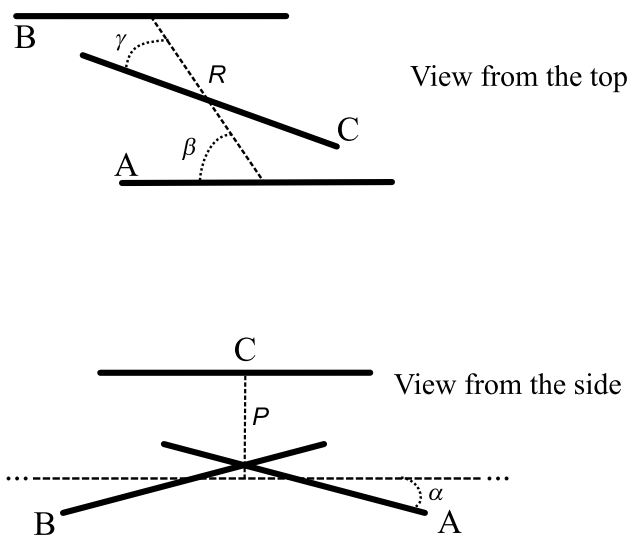


FIG. 6. Schematic illustration of the C_2 trimer. Molecules A and B are identical by symmetry and the distance between their centers is R . The perpendicular distance from the center of the line joining their centers to the center of molecule C is P .

TABLE VII. Energy well depth, U , equilibrium geometry and harmonic zero-point vibrational energy, E_0 , for the two most stable trimers predicted by the GCPCDO IP and the BUK IP. Because of uncertainties in the numerical Hessian, E_0 is rounded for the GCPCDO. The geometric variables are defined in Figure 6 for the C_2 minimum and in Figure 5 for the C_{3h} minimum.

	GCPCDO	BUK ^a
C_2 minimum		
U / K	-1849.4	-1889.8
E_0 / K	359	343.6
$R / \text{Å}$	3.73	3.60
$P / \text{Å}$	2.96	2.89
α / deg	12.1	10.9
β / deg	53.7	53.4
γ / deg	152.8	157.6
C_{3h} minimum		
U / K	-1849.4	-1819.6
E_0 / K	318	304.2
$R / \text{Å}$	4.07	4.04
β / deg	40.9	39.3

^a Ref. 2

shallow near the minimum so precision is difficult, and two different *ab initio* minimum energy geometries have been reported in the literature. Danten and collaborators⁵³ find that the energy minimum has C_s symmetry from counterpoise-corrected MP2 calculations with the aug-cc-pVTZ basis set. However, this is contested by both experimental^{54,55} and more high-level *ab initio* counterpoise-corrected calculations at the CCSD(T) level of theory and the same basis set which predict C_{2v} symmetry of the complex.⁵⁶ It is interesting to note that the MP2 level of theory often overestimates correlation effects, consistent with the fact that simple pair potentials, such as the ZD⁶ and TIP3P⁵² IPs under the Lorentz-Berthelot mixing rules, predict a C_{2v} minimum for the complex. The intermixing of the GCPCDO IP with GCPM water¹⁴ produces two, equivalent, global minima of C_s symmetry, but the

difference in energy between them and the transition state of C_{2v} symmetry connecting them is only about 7 K, *i. e.* less than 0.1% of the total interaction energy and should not be taken as great drawback of the model.

It is a greater error that the total binding energy is underestimated by about 25%, a fault shared by the ZD/TIP3P combination as well. This is surprising, because in general non-polarizable IPs parametrized against bulk properties tend to overestimate cluster binding energies. The explanation can partly be found in the rigid geometries of the GCPCDO/GCPM and ZD/TIP3P moieties. The results by Danten and coworkers⁵³ indicate that the CO₂ molecule is bent slightly upon complexation, thus further inducing a dipole moment which increases the energy of interaction. However, the greater part of the explanation is to be found in the approximation that only the central atom polarizes. A QM calculation at the CISD/aug-cc-pVDZ level of theory for the C_s minimum of the GCPM/GCPCDO complex indicate that while the total dipole moment of 2.19 D is in good agreement with the accurate value of 2.21 D, the individual components are poorly reproduced.⁵⁷ The QM calculation indicates that for the complex as a whole, the electric dipole moment along the C_2 axis of the water molecule is 2.16 D, and that the perpendicular component is 0.465 D in this particular configuration. The GCPM/GCPCDO pairing, however, indicates 2.19 D and 0.14 D, respectively, for these components. Further discrepancy is expected at the closer range indicated as the equilibrium distance by the *ab initio* calculations. In summary, as far as geometry and energy are concerned, the predictions of the GCPCDO/GCPM complex can hardly be considered an improvement over the simple empirical IPs, compared to *ab initio* calculations.

Despite this small short-coming of the predictions for the [CO₂-H₂O] complex, it is still worthwhile to consider the [(CO₂)₂-H₂O] complex, also studied by Danten and coworkers,⁵³ because here the true many-body interactions start to play a role. Moreover, contrary to the case of the CO₂ trimer, where none of the moieties is dipolar, the water molecule carries a substantial dipole moment and the electronic induction effects are expected to be more pronounced. It must be pointed out that despite this being a three-body system, no Axilrod-Teller potential has been applied. The reason is that while GCPM water has a known polarizability, it has no Axilrod-Teller coefficient. Rather than impose one on the model, I have decided to judge it fairly according to its own merits, and these exclude a three-body dispersion interaction. The results are shown in Table IX. The agreement is very good in

TABLE VIII. Minimum energy, U , and geometry of the $[\text{CO}_2\text{-H}_2\text{O}]$ complex as predicted by the mixing of GCPCDO and GCPM polarizable IPs, the ZD and TIP3P non-polarizable IPs, or *ab initio* calculation by Danten *et al.* at the MP2/aug-cc-pVTZ level of theory, or by Garden *et al.* at the CCSD(T)/aug-cc-pVTZ level of theory. The binding energy of the C_{2v} transition state predicted by the GCPCDO model is reported for completeness. For the definition of the geometry, see Figure 7.

	GCPCDO/GCPM		ZD/TIP3P	Danten ^a	Garden ^b
	C_s minimum	C_{2v} tr. state			
U / K	-1036.4	-1029.5	-1048.1	-1308.4	-1358.7
$R / \text{\AA}$	3.06	3.06	2.93	2.77	2.81
ϕ / deg	17.0	0.0	0.0	13.9	0.0
α / deg	87.4	0.0	0.0	88.0	0.0

^a Ref. 53

^b Ref. 56

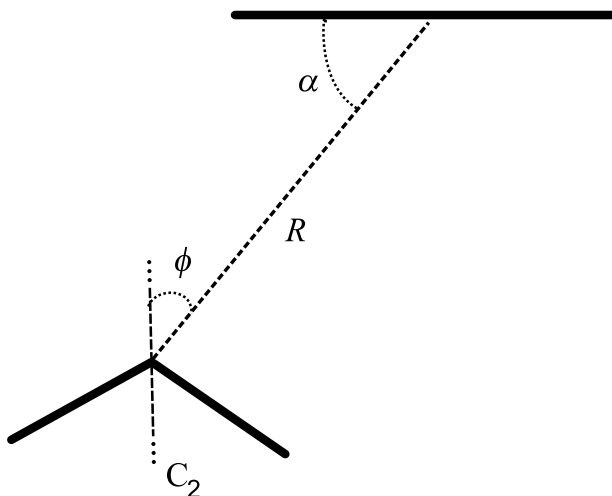


FIG. 7. Schematic illustration of the structure of the monohydrate complex. The C_2 axis of the water molecule is marked. All atoms lie in the same plane.

TABLE IX. Characteristics of the global minima of the $[(\text{CO}_2)_2-\text{H}_2\text{O}]$ complex predicted by the GCPCDO/GCPM IPs, the ZD/TIP3P IPs or the *ab initio* results of Danten *et al.* at the MP2/aug-cc-pVTZ level of theory. The oxygen of the water molecule is placed at the origin of a Cartesian coordinate system in which the y -axis coincides with the C_2 axis of the water molecule with the positive direction pointing toward the hydrogen atoms, the z -axis is normal to the molecular plane and the x -axis is orthogonal to the y - and z -axes. The centers of mass of the CO_2 molecules are given with respect to this coordinate system, and the orientation of each molecule is expressed in the Euler angles α , β and γ which denote counterclockwise rotation around the x -, y - and z -axes, respectively. U is the energy of that conformation. Indices 1 and 2 denote the two CO_2 molecules. The work in Ref. 53 used flexible molecules. The coordinates reported here are rounded over these differences.

	GCPCDO/GCPM	ZD/TIP3P	Danten ^a
Point group	C_s	C_2	C_s
U / K	-2738.5	-5074.0	-2918.7
x_1 / Å	0.00	-1.43	0.00
y_1 / Å	-2.61	-2.11	-2.52
z_1 / Å	1.58	-0.85	1.11
x_2 / Å	0.00	1.43	0.00
y_2 / Å	0.79	-2.11	0.42
z_2 / Å	3.80	0.85	3.80
α_1 / deg	53.7	-62.8	61.8
β_1 / deg	90.0	86.0	90.0
γ_1 / deg	90.0	-82.3	90.0
α_2 / deg	-69.1	62.8	-55.0
β_2 / deg	90.0	86.0	90.0
γ_2 / deg	90.0	82.3	90.0

^a Ref. 53

terms of energy. Contrary to the $[\text{CO}_2\text{--H}_2\text{O}]$ complex, for the $[(\text{CO}_2)_2\text{--H}_2\text{O}]$ complex, there is no appreciable underestimation of the binding energy. This can probably be attributed to the larger fraction of $\text{CO}_2\text{--CO}_2$ interactions in this complex. Moreover, both Danten *et al.*⁵³ and I find that the minimum is of C_s symmetry, but for the ZD⁶/TIP3P⁵² model, the global minimum is of C_2 symmetry in a conformation reminiscent of the C_2 trimer. A local minimum of C_2 symmetry is predicted by the GCPCDO/GCPM¹⁴ model at about 208 K above the global minimum. Clearly, polarization changes the relative stability of these two conformations in favor of the C_s one and this is captured both by the MP2 calculations of Danten *et al.*⁵³ and by the present work. The peculiarities of the global minima predicted by the IPs are given in Table IX. It is very clear that the many-body effects are responsible for the altered symmetry of the equilibrium structure. Also, the binding energy is vastly overestimated by the non-polarizable IP pair.

IV. CONCLUDING REMARKS

A new, polarizable IP for CO_2 has been introduced and shown to be in excellent agreement dimer properties and excellent-to-passable agreement for the bulk phase. Classical non-polarizable IPs that reproduce bulk phase properties well have been shown inadequate for the description of $B_2(T)$ and also $B_3(T)$. That many-body effects should not be ignored for the CO_2 molecule is evidenced by the qualitative experimental agreement that is achieved for the stability of the two trimer conformations, something which not even the *ab initio* potential energy surface of Bukowski *et al.*² manages. Further corroboration of the model is provided by calculations on the water complexes, where especially the $[(\text{CO}_2)_2\text{--H}_2\text{O}]$ complex is in good agreement with *ab initio* calculation at the MP2/cc-aug-pVTZ level of theory.⁵³ Absence of polarization changes the symmetry of this complex.

A tough test for all of the molecular CO_2 potentials investigated is the prediction of the virial coefficients. The GCPCDO model handles $B_2(T)$ and $B_3(T)$, but only because of design, and fails at $B_4(T)$ and up. This can still be considered an improvement over the classical, non-polarizable models for which most probably none of the virial coefficients beyond the ideal gas term are in agreement with experiment. Clearly, the interaction among CO_2 molecules is more complicated than a simple pairwise sum over atomic charges and Lennard-Jones terms. However, it is also more complicated than self-consistent solution of

induced dipoles and triple-dipole dispersion interaction. Nevertheless, for systems of three bodies or less, it seems to be highly satisfactory, meaning that the remaining errors relate to many-body effects beyond the third. On the precise causes of the remaining errors in the IP can only be speculated and future computer experiments may provide the answer to what the mechanisms are.

It is in this light that it must be kept in mind that even if in comparison with experiment, the GCPCDO model, with a few exceptions, rests more on qualitative concordance than on many digits of precision, this is the first many-body molecular IP for the CO₂ molecule to be developed and that many areas of inquiry remain to explore. One obvious and immediate improvement to the model would be to distribute the induced dipole over all atoms for a better short-range description of the induced electrostatics.

The Fortran 90 source code for the GCPCDO energy subroutines is available upon request.

ACKNOWLEDGMENTS

The simulations were performed on the C3SE computing resources. The author also wishes to express his gratitude to Prof. Robert Bukowski for granting him the BUK subroutines and to Prof. Sture Nordholm for insightful comments on the manuscript. Serious errors were noted by the anonymous reviewers and the author is highly indebted to both.

REFERENCES

- ¹G. Steinebrunner, A. J. Dyson, B. Kirchner, and H. Huber, *J. Chem. Phys.* **109**, 3153 (1998).
- ²R. Bukowski, J. Sadlej, B. Jeziorski, P. Jankowski, K. Szalewicz, S. A. Kucharski, H. L. Williams, and B. M. Rice, *J. Chem. Phys.* **110**, 3785 (1999).
- ³S. Bock, E. Bich, and E. Vogel, *Chem. Phys.* **257**, 147 (2000).
- ⁴J. J. Potoff and A. Z. Panagiotopoulos, *J. Chem. Phys.* **109**, 10914 (1998).
- ⁵J. Vrabc, J. Stoll, and H. Hasse, *J. Phys. Chem. B* **48**, 12126 (2001).
- ⁶Z. Zhang and Z. Duan, *J. Chem. Phys.* **122**, 214507 (2005).

- ⁷C. S. Murthy, K. Singer, and I. R. McDonald, *Mol. Phys.* **44**, 135 (1981); C. S. Murthy, S. F. Oshea, and I. R. McDonald, *ibid.* **50**, 531 (1983).
- ⁸A. Koide and T. Kihara, *Chem. Phys.* **5**, 34 (1974).
- ⁹T. B. MacRury, W. A. Steele, and B. J. Berne, *J. Chem. Phys.* **64**, 1288 (1976).
- ¹⁰J. G. Harris and K. H. Yung, *J. Phys. Chem.* **99**, 12021 (1995).
- ¹¹T. Merker, C. Engin, J. Vrabc, and H. Hasse, *J. Chem. Phys.* **132**, 234512 (2010).
- ¹²T. Merker, J. Vrabc, and H. Hasse, *J. Chem. Phys.* **129**, 087101; author reply 087102 (2008).
- ¹³B. M. Axilrod and E. Teller, *J. Chem. Phys.* **11**, 299 (1943).
- ¹⁴P. Paricaud, M. Predota, A. A. Chialvo, and P. T. Cummings, *J. Chem. Phys.* **122**, 244511 (2005).
- ¹⁵A. A. Chialvo and P. T. Cummings, *Fluid Phase Equilib.* **150**, 73 (1998).
- ¹⁶G. Maroulis, *Chem. Phys.* **291**, 81 (2003).
- ¹⁷N. J. Bridge and A. D. Buckingham, *Proc. R. Soc., Ser. A* **295**, 334 (1966).
- ¹⁸A. Chrissanthopoulos, U. Hohm, and U. Wachsmuth, *J. Mol. Struct.* **526**, 323 (2000).
- ¹⁹P. Ahlström, A. Wallqvist, S. Engström, and B. Jönsson, *Mol. Phys.* **68**, 563 (1989).
- ²⁰B. M. Axilrod, *J. Chem. Phys.* **19**, 719 (1951).
- ²¹P. Atkins and R. Friedman, *Molecular Quantum Mechanics*, 4th ed. ed. (Oxford University Press, Oxford, 2005).
- ²²M. D. Harmony, V. W. Laurie, R. L. Kuczkowski, R. H. Schwendeman, and D. A. Ramsay, *J. Phys. Chem. Ref. Data* **8**, 619 (1979).
- ²³G. Granar, C. Rossetti, and D. Bailly, *Mol. Phys.* **58**, 627 (1986).
- ²⁴A. D. Buckingham and R. L. Disch, *Proc. Roy. Soc. A* **273**, 275 (1963).
- ²⁵J. E. Harries, *J. Phys. B: At. Mol. Phys.* **3**, L150 (1970).
- ²⁶R. Eisenschitz and F. London, *Z. Phys.* **60**, 491 (1930).
- ²⁷J. K. Singh and D. A. Kofke, *Phys. Rev. Lett.* **92**, 220601 (2004).
- ²⁸J. M. Flega, M. Haran, and G. L. Jones, *Statist. Sci.* **23**, 250 (2008).
- ²⁹W. Dushek, R. Kleinrahm, and W. Wagner, *J. Chem. Thermodyn.* **22**, 827 (1990).
- ³⁰J. C. Holste, K. R. Hall, P. T. Eubank, G. Esper, M. Q. Watson, W. Warowny, D. M. Bailey, J. G. Young, and M. T. Bellomy, *J. Chem. Thermodyn.* **19**, 1233 (1987).
- ³¹P. J. Leonard and J. A. Barker, "Theoretical Chemistry: Advances and Perspectives," (Academic Press, New York, 1975) Multiply the referenced value by the polarizability of argon for the cited one.

- ³²N. Metropolis, A. W. Rosenbluth, M. N. Rosenbluth, A. N. Teller, and E. Teller, *J. Chem. Phys.* **21**, 1087 (1953).
- ³³L. Onsager, *J. Am. Chem. Soc.* **58**, 1486 (1936).
- ³⁴F. G. Keyes and J. G. Kirkwood, *Phys. Rev.* **36**, 754 (1930).
- ³⁵D. Frenkel and B. Smit, *Understanding molecular simulations*, 2nd ed. (Academic Press, 2001).
- ³⁶V. Eyert, *J. Comp. Phys.* **124**, 271 (1996).
- ³⁷R. Pengyu and J. W. Ponder, *J. Phys. Chem. B* **107**, 5933 (2003).
- ³⁸J. J. Potoff and J. I. Siepmann, *AIChE J.* **47**, 1676 (2001).
- ³⁹T. L. Hill, *Statistical mechanics: Principles and selected applications*, 2nd ed. (MacGraw-Hill Book Company, New York, 1956).
- ⁴⁰P. E. Martin and E. F. Barker, *Phys. Rev.* **41**, 291 (1932).
- ⁴¹Y. Ouazzany and J. P. Boquillon, *Europhys. Lett.* **4**, 421 (1987).
- ⁴²E. W. Lemmon, M. O. McLinden, and D. G. Friend, "NIST Chemistry WebBook, NIST Standard Reference Database Number 69," (National Institute of Standards and Technology, Gaithersburg MD, 20899, 2008) Chap. Thermophysical Properties of Fluid Systems, <http://webbook.nist.gov>, (retrieved August 5, 2010).
- ⁴³P. Cipriani, M. Nardone, and F. P. Ricci, *Physica B* **241-243**, 940 (1998).
- ⁴⁴J. B. van Tricht, H. Fredrikze, and J. van der Laan, *Mol. Phys.* **52**, 115 (1984).
- ⁴⁵A. E. Barton, A. Chablo, and B. J. Howard, *Chem. Phys. Lett.* **60**, 414 (1978).
- ⁴⁶M. A. Walsh, T. H. England, T. R. Dyke, and B. J. Howard, *Chem. Phys. Lett.* **142**, 265 (1987).
- ⁴⁷B. Jeziorski, R. Moszynski, and K. Szalewicz, *Chem. Rev.* **94**, 1887 (1994).
- ⁴⁸M. J. Frisch, G. W. Trucks, H. B. Sclegel, G. E. Scuseria, M. A. Robb, J. R. Cheeseman, J. A. Montgomery, Jr., T. Vreven, K. N. Kudin, J. C. Burant, J. M. Millam, S. S. Iyengar, J. Tomasi, V. Barone, B. Mennucci, M. Cossi, G. Scalmani, N. Rega, G. A. Petersson, H. Nakatsuji, M. Hada, M. Ehara, K. Toyota, R. Fukuda, J. Hasegawa, M. Ishida, T. Nakajima, Y. Honda, H. Kitao, O. and Nakai, M. Klene, X. Li, J. E. Knox, H. P. Hratchian, J. B. Cross, V. Bakken, C. Adamo, J. Jaramillo, R. Gomperts, R. E. Stratmann, O. Yazyev, A. J. Austin, R. Cammi, C. Pomelli, J. W. Ochterski, P. Y. Ayala, K. Morokuma, G. A. Voth, P. Salvador, J. J. Dannenberg, V. G. Zakrzewski, S. Dapprich, A. D. Daniels, M. C. Strain, O. Farkas, D. K. Malick, A. D. Rabuck, K. Raghavachari,

- J. B. Foresman, J. V. Ortiz, Q. Cui, A. G. Baboul, S. Clifford, J. Cioslowski, B. B. Stefanov, G. Liu, A. Liashenko, P. Piskorz, I. Komaromi, R. L. Martin, D. J. Fox, T. Keith, M. A. Al-Laham, C. Y. Peng, A. Nanayakkara, M. Challacombe, P. M. W. Gill, B. Johnson, W. Chen, M. W. Wong, C. Gonzalez, and J. A. Pople, *Gaussian 03, Revision E.01*, Wallingford, CT (2004).
- ⁴⁹M. J. Weida, J. M. Spherac, and D. Nesbitt, *J. Chem. Phys.* **103**, 7685 (1995).
- ⁵⁰M. J. Weida and D. Nesbitt, *J. Chem. Phys.* **105**, 10210 (1996).
- ⁵¹The precise value of this difference is uncertain because of the numerical minimization involved, but my program code indicates that the C_2 conformation lies 0.03 K above the C_{3h} one.
- ⁵²W. L. Jorgensen, J. Chandrasekhar, J. D. Madura, R. W. Impey, and M. L. Klein, *J. Chem. Phys.* **79**, 926 (1983).
- ⁵³Y. Danten, T. Tassaing, and M. Besnard, *J. Phys. Chem. A* **109**, 3250 (2005).
- ⁵⁴K. I. Peterson and W. J. Klemperer, *J. Chem. Phys.* **80**, 2439 (1984).
- ⁵⁵T. L. Tso and E. K. C. Lee, *J. Phys. Chem.* **89**, 1612 (1985).
- ⁵⁶A. L. Garden, J. R. Lane, and H. G. Kjaergaard, *J. Chem. Phys.* **125**, 144317 (2006).
- ⁵⁷It must be remembered, however, that a large part of this dipole moment is due to the ground-state charge distribution of the water molecule, captured already by the partial charges in the GCPM water.